41st AIAA/ASME/ASCE/AHS/ASC Structures, Structural Dynamics, and Materials Conference and Exhibit
Atlanta, GA 3-6 April 2000

A00-24567

AIAA 2000-

Dynamic Taxi, Take-Off and Landing Roll Analyses for Large Business Jet Aircraft

Donald Freund[†], Douglas R. McKissack[*], Laurence C. Hanson[§], and Hank Brodman[‡]

Loads & Dynamics
Gulfstream Aerospace Corporation
Savannah, GA 31402-2206

Abstract

The FAA/JAA draft Advisory Circular (AC) pertaining to taxi, take-off, and landing roll design loads identifies dynamic analyses using random runway and tuned bump ground profiles. The large business jet model used to evaluate the requirements of the AC is comprised of experimentally validated landing gear and airframe models, which are mated in DADS®, a commercially available non-linear dynamics software package. The results presented from this study focus on landing gear ground reactions, with secondary areas of interest that include the fuselage, wing, and nacelle loads. In addition, factors impacting simulation run-times will be addressed.

Introduction

The dynamic loads arising from aircraft operation on the roughest runway or taxiway expected in normal service must not compromise the structural integrity of the airframe or landing gear for transport aircraft. A test program involving an instrumented aircraft and suitably rough runway may satisfy this requirement. However, an experimental program of this nature would require a sizable effort to locate and survey candidate runways or fabricate artificial roughness on an existing runway. In addition, a substantial operating cost would be incurred during the testing of various combinations of speed, aircraft weight, center of gravity, etc. In today's lean aircraft companies, tests of this nature are prohibitively expensive thereby requiring an alternative means of compliance, such as by computer simulation. Current leading-edge computer platforms and structural dynamics software packages are sufficient to solve problems such as these, and require a fraction of the resources relative to full-scale testing.

The certification requirements set forth in FAR/JAR 25.491 can be addressed by the methodology set forth in pending Advisory Circular (AC) 25.491-1[1]. The AC describes three separate analyses including a runway (random) profile, a discrete (tuned bump or 1.7g static), and main gear combined load conditions which can be used to show compliance. The runway profile and tuned bump analyses involve dynamic analyses of the aircraft over the respective ground profiles. The main gear combined load condition is a formula condition based on the loads generated by the discrete load condition.

Model Attributes and Aircraft Conditions

The AC requires certain attributes to be included in the dynamic model, such as: important flexible airframe modes, landing gear dynamics and tire characteristics, and rigid body aerodynamics (aeroelastic effects may be ignored). The AC also specifies that runs should be performed at maximum takeoff gross weight (MTOW) and maximum landing gross weight (MLGW), taking into account center of gravity (CG) extremities. Engine thrust for MTOW

[†] Dynamics Engineer, Member AIAA. E-mail: don.freund@gulfaero.com
[*] Loads & Dynamics Technical Specialist, Associate Fellow AIAA. E-mail: doug.mckissack@gulfaero.com
[§] Loads & Dynamics Manager, Associate Fellow AIAA. E-mail: larry.hanson@gulfaero.com
[‡] Loads & Dynamics Group Head, Senior Member AIAA. E-mail: hank.brodman@gulfaero.com.

cases (or reverse thrust for MLGW cases) should be considered if critical. For MLGW runs, braking must be simulated by steady pitching moments generated by a coefficient of friction of 0.3.

In lieu of performing take-off or landing roll transients, constant speed runs are specified to ensure that critical areas of the runway are traversed. The speed range includes from 20 knots up to rotation speed (V_R) and maximum landing speed (1.25 V_{L2}) for MTOW and MLGW runs, respectively, which are to be evaluated on the ground profiles discussed in the following.

Runway Profile Condition

The runway profile specified in the AC is the San Francisco International Airport 28R (SF28R) as it existed in the early 1960's[2]. High aircraft loadings and subsequent pilot complaints were generated during operations on this runway, therefore, the runway was resurfaced. There are other runway data available in Refs. 3-4. The SF28R profile (before it was resurfaced) is shown in Fig. 1a, with the elevation datum shifted down 10.3 ft. The runway length is 3880 ft with elevation data is available in 2 ft. longitudinal increments.

A preliminary evaluation of the SF28R runway indicated that one 12 ft. segment of the runway was shifted up approximately 0.1 ft. relative to adjacent points (shown in Fig. 1b). The 0.1 ft. shift may be either temporary asphalt patch or a measurement/report error (an error with identical nature was rectified at an another location on this runway). Since the points exceed the current runway roughness standards, a proposal has been developed using the 1.0% maximum slope change specified in the ICAO Annex 14 temporary ramp specifications[5]. The modification is shown in Fig. 1b. Note that the ICAO standard is more liberal than the FAA counterpart, which limits slope changes for temporary ramps to 0.566%[6].

Bi-directional runs are required on the San Francisco runway to ensure that directionally dependent runway structures are traversed (i.e. a sharp fall-off in one direction may be an abrupt bump in the other direction).

Discrete Profile Condition

As an alternative to a 1.7g static condition, the AC states that the aircraft response to double tuned bumps (on an otherwise smooth runway) may be investigated under the same conditions considered for the SF28R analysis. The bump wavelengths (λ) are to be equal to the longitudinal distance between the nose and main gears ($\lambda=L$), and twice this distance ($\lambda=2L$). These wavelengths were chosen to excite the aircraft plunge and pitch rigid body modes, respectively. The bump amplitude (H, in inches) for each case is specified as

$$H(\lambda) = 1.2 + 0.023\sqrt{\lambda} \qquad [1]$$

where λ is in inches. This formula was extracted from the Air Force double tuned bump criteria for prepared surfaces[7].

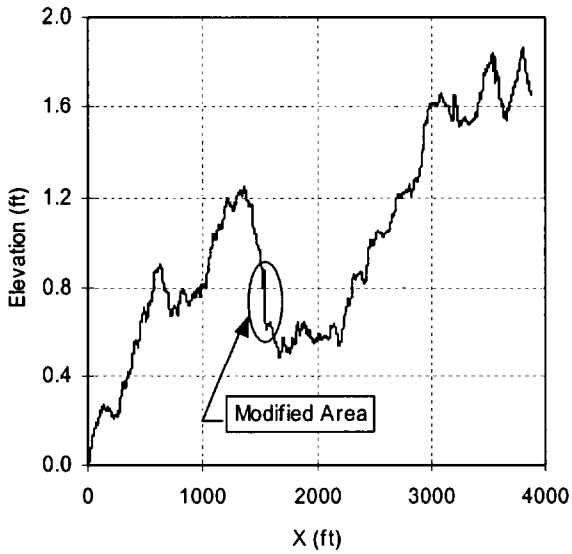

(a) SF28R

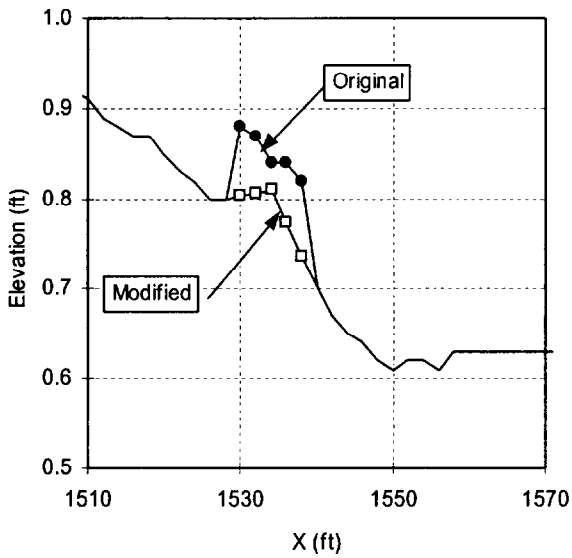

(b) modified bump on SF28R

Fig. 1 - San Francisco runway profile.

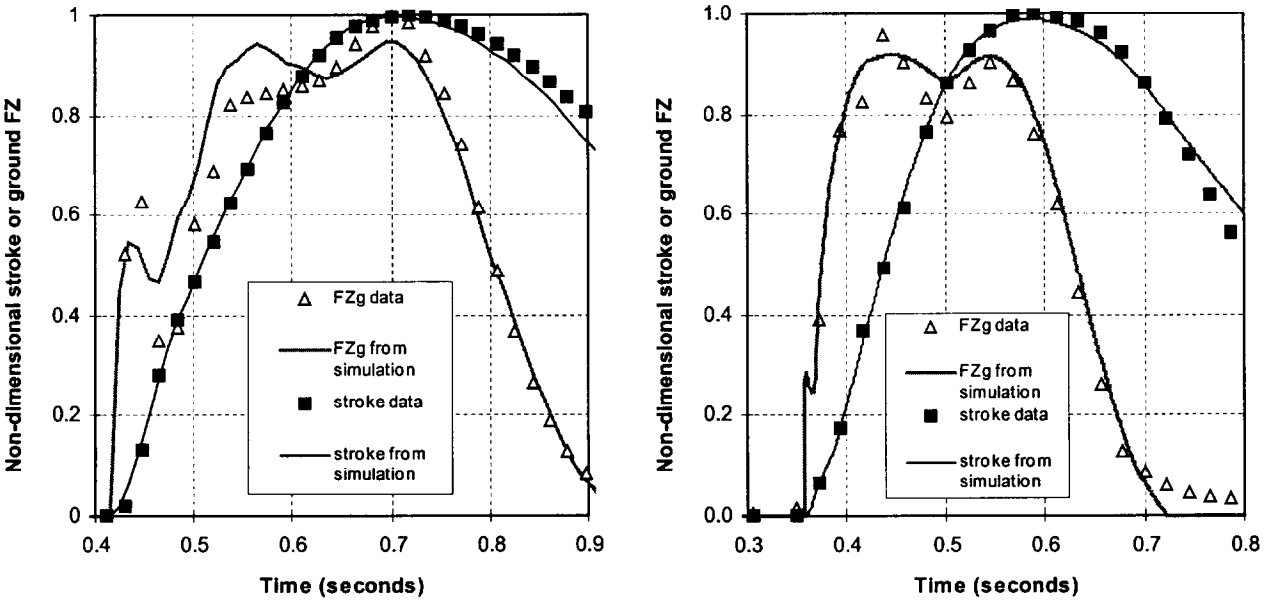

Fig. 2 - Stroke and vertical ground reaction from simulations compared against drop test data.

The remainder of this paper focuses on the methodology used to create a taxi model and on the landing gear/airframe loads generated using the runway and tuned bump ground profiles. Factors impacting simulation performance will be also be addressed.

Taxi Model

Since the published elevation profile of SF28R and tuned bump amplitudes vary in the longitudinal direction only, it is appropriate to use a half-airplane model for these analyses, with symmetric boundary conditions applied along the centerline. The model consists of a flexible airframe model mated with one main landing gear model and a half-nose gear model. Brief descriptions of each component are contained in the following.

Gear Models

The main landing gear is an oleo-pneumatic type with an articulated, trailing arm axle with two 35 inch diameter tires. The nose gear is a oleo-pneumatic, cantilevered design with 21 in. diameter tires. Both main and nose gears use a metering pin to optimize strut efficiency during landings.

The gear can be accurately modeled by including the mass properties, strut flexibility, tire and oleo-pneumatic characteristics. Although DADS does not have a force element specifically designed for oleo-pneumatic struts, the air, oil, and frictional forces can be easily modeled using general control elements. The strut force is a non-linear function of stroke (s) and stroke velocity ($\dot{s}$), and can be written as

$$F_{strut}(s,\dot{s}) = A_{N_2} p_{N_2}(s) + A_{oil}\Delta p_{oil}(s,\dot{s}) + F_{seal}(\dot{s}) \quad [2]$$

where:

$$p_{N_2}(s) = -p_{amb} + (p_o + p_{amb})\left(\frac{V_o - sA_{N_2}}{V_o}\right)^{\gamma} \quad [3a]$$

$$\Delta p_{oil} = \frac{\rho_{oil}\dot{s}^2}{2K^2}\frac{(A_{oil} - A_{pin}(s))}{(A_{orif} - A_{pin}(s))} \quad [3b]$$

with design dependent variables of V for volume, A for cross-sectional area, p for pressure, and ρ for density. The subscripts N_2, *amb*, *o*, *oil*, *pin*, and *orif* indicate pneumatic, ambient, fully-extended, hydraulic, metering pin, and orifice values, respectively.

The air-spring exponent (γ), seal friction term (F_{seal}) and flow coefficient (K) selected represent a best fit of all the experimental drop test data at a variety of weights, attitudes, and sink weights for each respective gear model.

Figures 2a and b show normalized stroke and vertical ground reaction (FZ) from a DADS drop test simulation compared against test data for the main and nose gear, respectively. The data shown (for each gear) represents one of several weight/sink rate combinations evaluated. The stroke and vertical ground reactions are

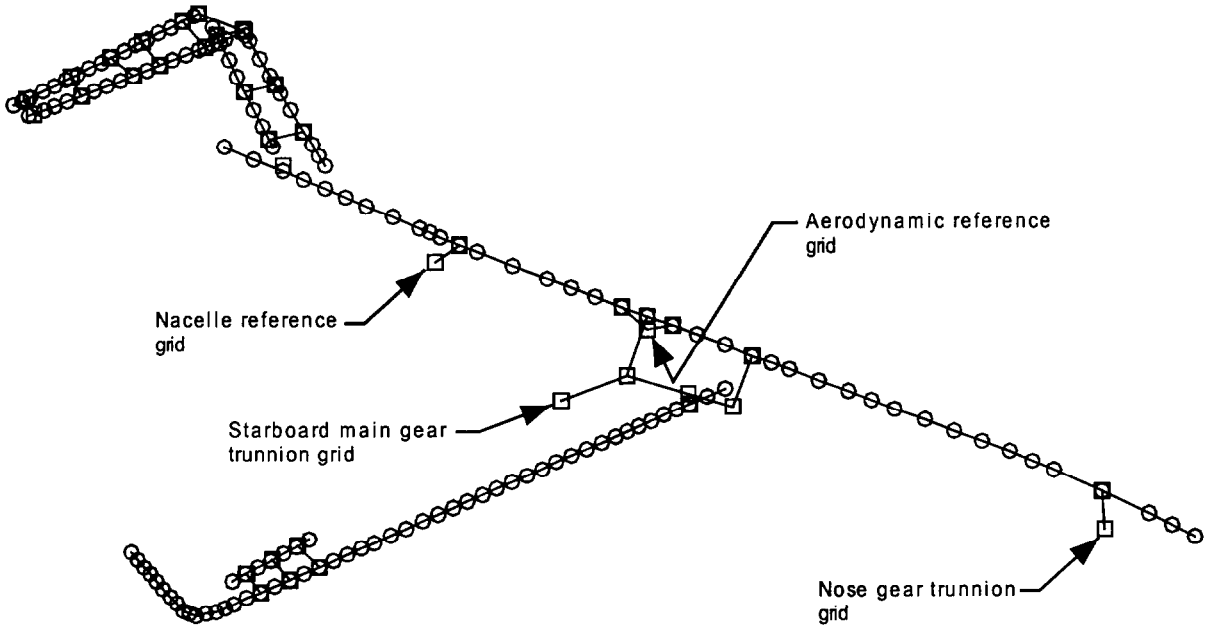

Fig. 3 - NASTRAN "stick" half-model.

normalized against the respective peaks from the test data. It is evident that the simulations closely predict the shape and magnitude of stroke for each respective gear model. In addition, the simulations adequately capture the large-scale features and magnitudes of FZ data.

Airframe Model

The airframe model was created with MSC®/NASTRAN® using a lumped mass system connected by variable property beams, known as a stick model. The flexible modes of primary importance are wing first bending, fuselage first bending, etc. which are accurately modeled by the stick model (within ±2% of ground vibration test results).

The airframe stick model geometry (shown in Fig. 3), mass, stiffness, and modal information were calculated in NASTRAN SOL 103 and output into files suitable for importation into the DADS flexible body translator. The first 20 symmetric flexible modes were used.

Gear Attachment and External Force Application to Airframe Body

The main and nose gear are attached to grid points corresponding to the respective trunnions (locations shown in Fig. 3). Rigid body aerodynamics and engine thrust are applied to grid points corresponding to the aerodynamic and nacelle reference grids, respectively, also shown in Fig. 3.

Computed Rigid Body Natural Frequencies for the Aircraft Resting on the Gear

A simple two-degree (plunge and pitch) of freedom system was utilized to evaluate the rigid-body natural frequencies (f) of the aircraft resting on it's gear. In this system, the airframe is represented as a rigid body, with mass m and pitch inertia I, and the nose and main landing gear as linear springs, with stiffness k_M and k_N, respectively. The equations of motion are:

$$m\ddot{z} + (k_M + k_N)z + (k_M L_M - k_N L_N)\theta = 0 \qquad [4a]$$

$$I\ddot{\theta} + (k_M L_M - k_N L_N)z + (k_M L_M^2 + k_N L_N^2)\theta = 0 \qquad [4b]$$

The variables z, θ, L_M and L_N are defined in Fig. 4. Assuming harmonic motion, the natural frequencies of the system can be written as:

$$f_1 = \frac{-b - \sqrt{b^2 - 4ac}}{4\pi a} \qquad [5a]$$

$$f_2 = \frac{-b + \sqrt{b^2 - 4ac}}{4\pi a} \qquad [5b]$$

where:

$$a = mI \qquad [6a]$$

$$b = -m(k_M L_M + k_N L_N) - I(k_M + k_N) \qquad [6b]$$

$$c = k_M k_N (L_M + L_N)^2 \qquad [6c]$$

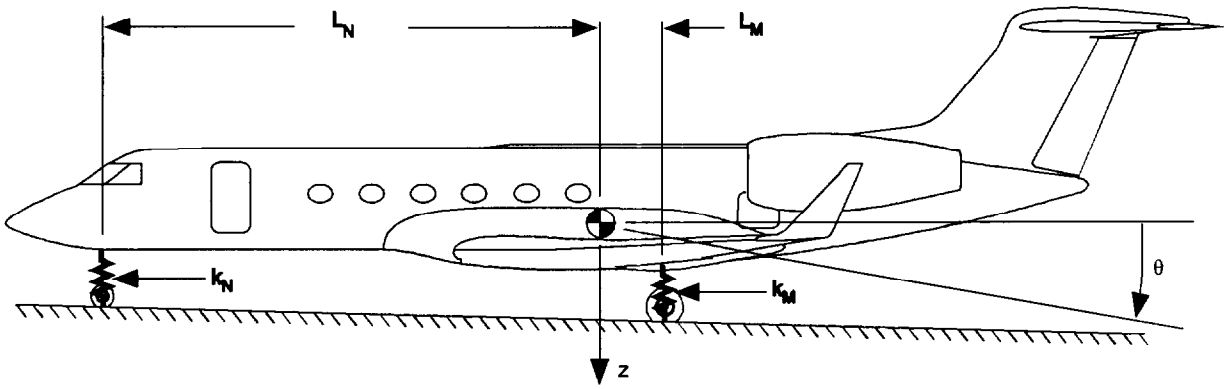

Fig. 4 - Two degree of freedom spring-mass system used to determine rigid body natural frequencies.

It should be noted that the linear spring constants k_M and k_N represent the equivalent strut/tire stiffness. In addition, both main gear are lumped into k_M.

The natural frequencies corresponding to MTOW (90900 lbs) and MLGW (75300 lbs) were found to be [f_1=1.27 Hz, f_2=1.49 Hz] and [f_1=1.30 Hz, f_2=1.50 Hz], respectively.

The fundamental oscillatory motion (pitch&plunge) of the aircraft model was compared against the computed natural frequencies to ensure that the gross behavior is appropriate, as discussed in the following.

Results

In lieu of running numerous combinations of weight, CG, thrust, braking, etc, two configurations were selected that produce the highest respective steady loading on the main and nose gear. For the main gear, the most critical combination was found to be at MTOW with extreme aft CG. Although this is a take-off configuration, engine thrust was not applied as it relieves the loading on the main gear. For the nose gear, the critical combination was found to be a braking

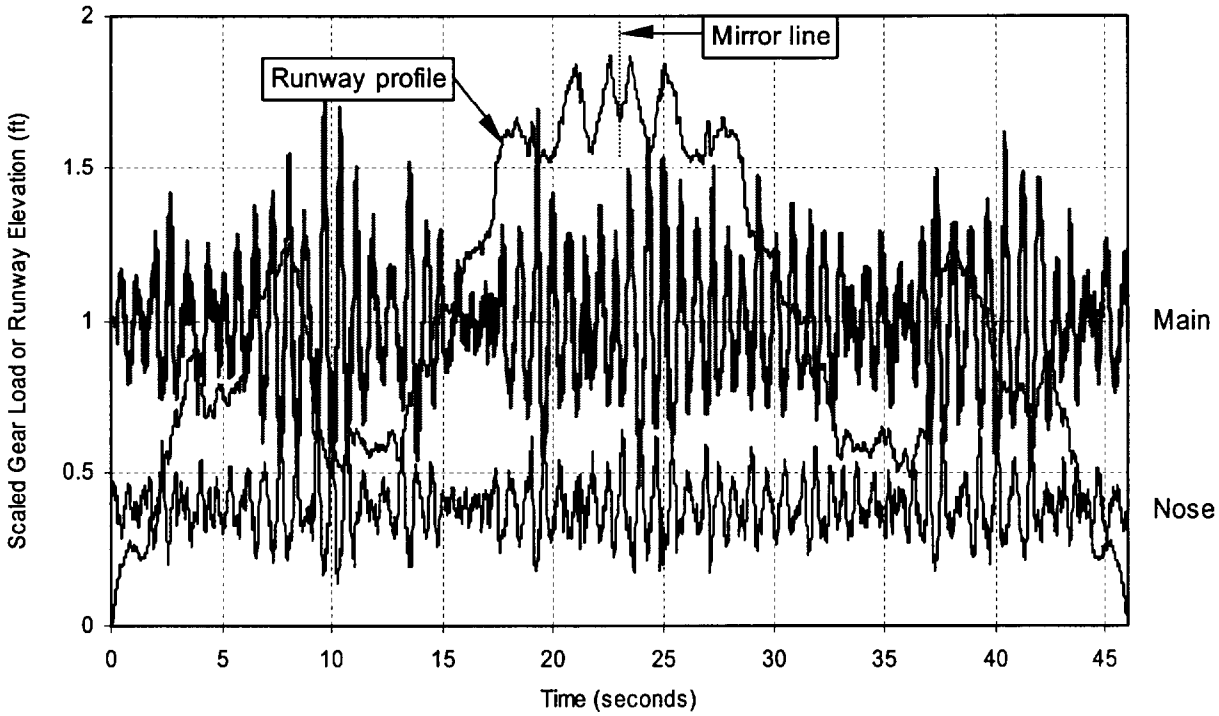

Fig. 5 - Typical SF28R main and nose gear loads. Constant speed run at MLGW (extreme forward CG) with steady braking. Gear loads are normalized by the steady main gear load.

condition at MLGW with extreme forward CG. Reverse thrust was not included as it relieves the loading on the nose gear.

Constant speed runs were made from 20 knots up to V_R and $1.25V_{L2}$ for the MTOW and MLGW configurations, respectively, in 20 knot increments. Rigid body aerodynamics were included, which reflect flap and spoiler settings approved for normal operation at MTOW or MLGW.

Figure 5 shows a typical time-history of main and nose gear loads generated on SF28R. Since bi-directional runs are required, the runway profile was mirrored about the end at x=3880 ft, resulting in the traverse of 7760 ft per run. It is evident in Fig. 5 that there is a well-defined oscillation (1.33 Hz) present in the main and nose gear load time-histories, which is attributed to the rigid body motion of the aircraft. This result is in excellent agreement with the computed natural frequency (f_1) of 1.30 Hz for this weight and CG.

Figure 6 shows a 4 second segment of the gear loads (extracted from Fig. 5), to illustrate the impact of the severe bump (shown in Fig. 1b) on nose gear loads. As shown in Fig. 6, the aircraft rigid body motion produces a compression of the nose gear (relative to the steady position) during the traverse, thereby reducing the amount of nose strut and tire deflection available to absorb the severe bump. The net result is a sharp peak in the nose gear load.

Figure 7 shows the temporal history of main and nose gear loads from a typical tuned bump simulation ($\lambda=L$) at MTOW with aft CG. At this wavelength, the rigid body plunge mode is excited during the traverse of the bumps. After the bumps have been traversed, the aircraft very quickly transitions into a 1.22 Hz combined pitch/plunge mode on the smooth segment of runway following the bumps. The computed natural frequency (f_1) for this weight and GC is 1.27 Hz, which is in close agreement with the simulation result. It should be noted that for this case, the maximum main gear load occurs on the smooth segment of runway *proceeding* the bumps.

Maximum Gear Loads - SF28R

The maximum main and nose gear loads arising from bi-directional runs on the San Francisco runway are shown in Figs. 8a and b, respectively. The main gear load is shown to increase moderately with ground speed (V), with the highest load occurring at V_R. For the nose gear, a trend is not readily interpreted, as there are four points of near maximum magnitude scattered in the data. These points are attributed to nose gear traversing the severe bump (e.g. Fig. 6), with worst

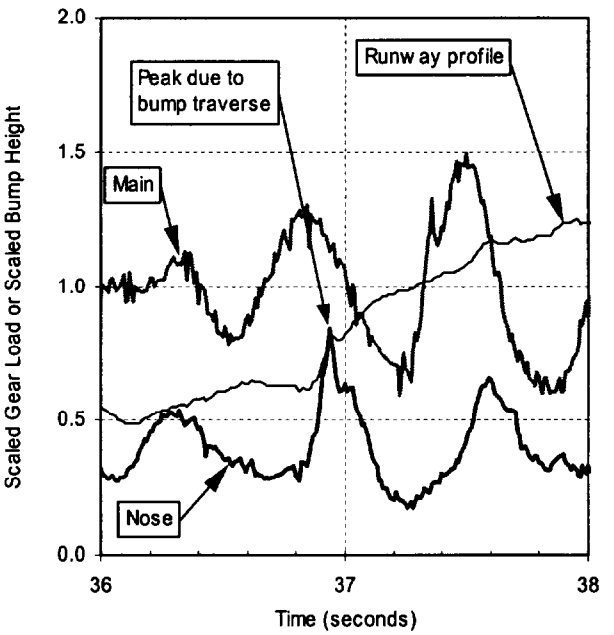

Fig. 6 - Close-up of SF28R scaled main and nose gear loads around the critical bump. Constant speed run at MLGW with extreme forward CG.

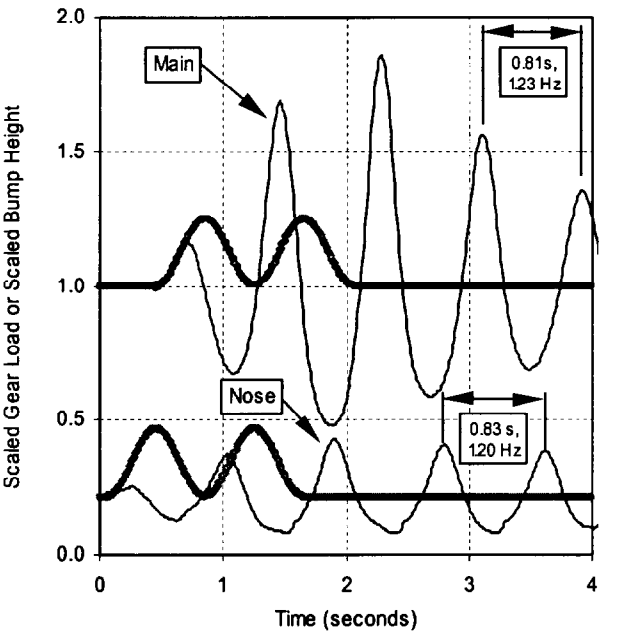

Fig. 7 - Typical tuned bump main and nose gear loads. Constant speed run at MTOW with aft CG. Bump wavelength (λ) = $2L$. Respective temporal positions of bump profile shown for main and nose gear.

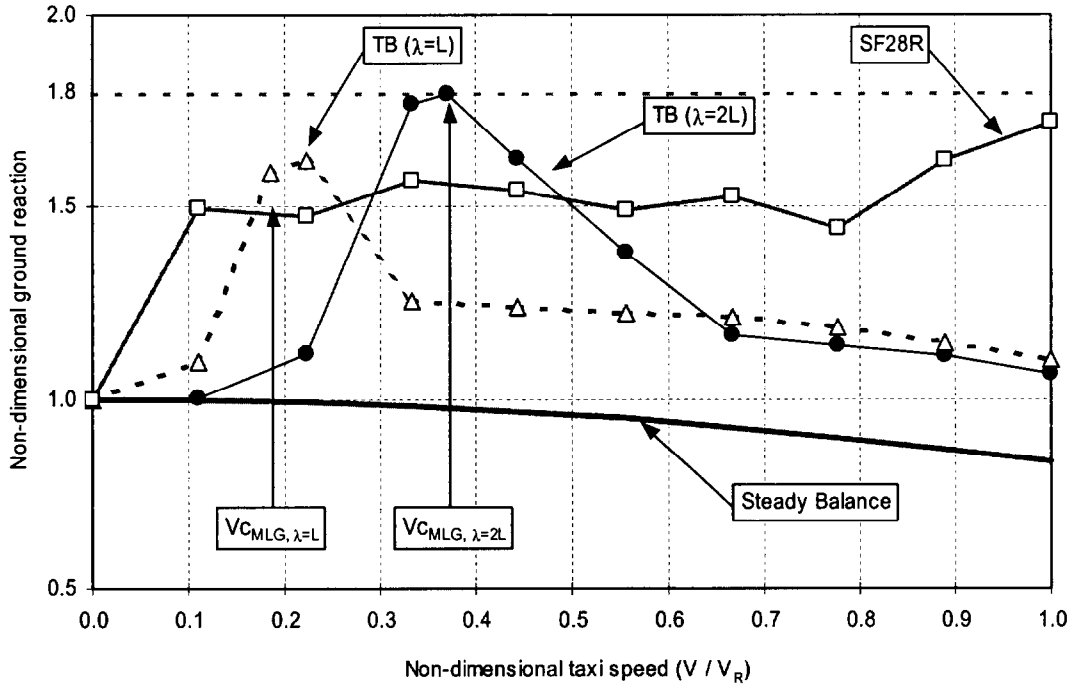

(a) Main landing gear - MTOW, aft CG, no thrust

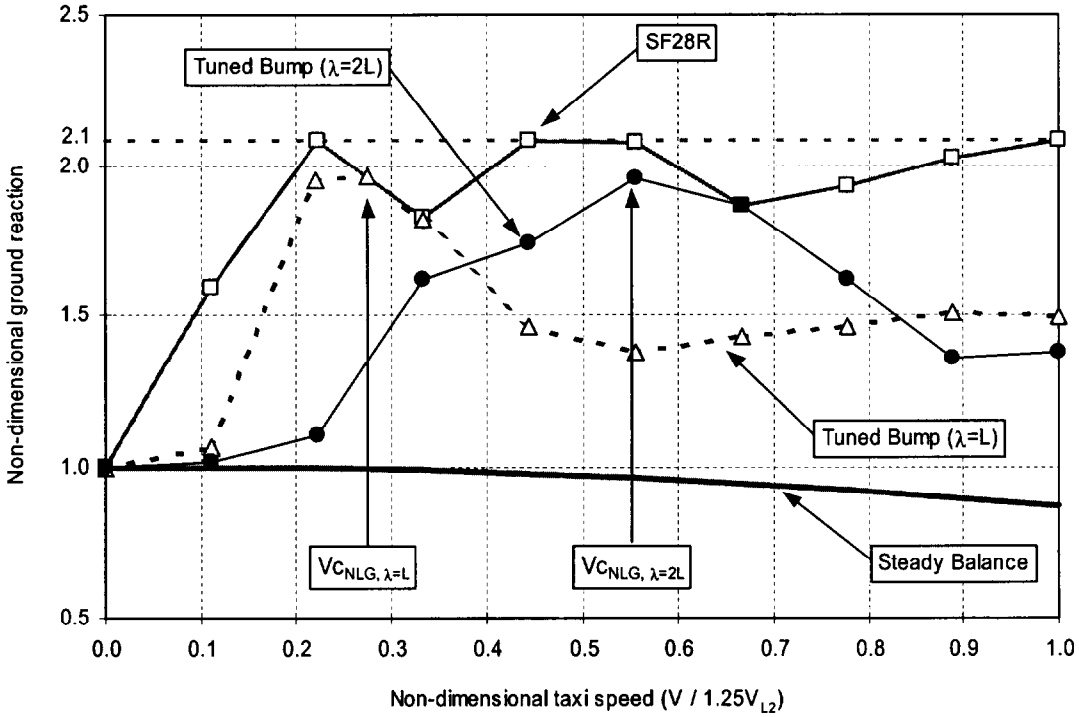

(b) Nose landing gear - MLGW, forward CG, steady braking, no reverse thrust

Fig. 8 - Gear loads from double tuned bumps and San Francisco runway.

possible phasing due to the rigid body pitch/plunge motion.

Maximum Gear Loads - Tuned Bump

Knowing the fundamental rigid body behavior prior to performing the tuned bump analysis provides insight as to the selection of critical speeds. For the main gear, the traverse speed which excites the fundamental rigid body pitch/plunge mode is defined to be the critical speeds ($Vc_{MLG} = \lambda f_1$). At this speed, it was determined that the CG of the aircraft experiences the highest accelerations during the traverse of the bumps. A second critical speed can be defined for the nose gear which results in the pitch motion of the aircraft being 180° out of phase with the peak of the second bump ($Vc_{NLG} = 1.5\ \lambda f_1$). Figures 8a and b also show the peak gear loads from the $\lambda = L$ and $2L$ tuned bump runs (indicated as TB($\lambda = L$) and TB($\lambda = 2L$), respectively), which were performed at the same speed increments, weights, CGs, etc. as for the San Francisco runway. It is evident that the tuned bump peak main and nose gear loads occur on (3 out of 4) or very near the respective critical speeds. In addition, the main and nose gear loads decrease significantly as V increases above Vc, which is attributed to the gear 'floating' over the second bump.

Fuselage Loads

Fuselage loads were computed from all of the SF28R and tuned bump runs via a post-processing routine. Aircraft rigid body and modal accelerations extracted from the dynamic simulations were converted into incremental inertial loads and summed with 1g inertial loads plus externally applied loads (i.e. main and nose trunnion loads and wing, nacelle, and empennage attach loads). Aerodynamic loads on the fuselage are assumed to be negligible. Note: forward fuselage loads are integrated from the nose aft.

The integrated shear and bending limit loads generated by runs on SF28R and tuned bump are plotted against the design values from flight and/or other ground conditions in Fig. 9 for nine stations. Note that the shear and bending values are normalized against the respective fuselage maxima. It is evident that the taxi loads are generally much less than the design cases, except in the forward fuselage stations where the taxi loads approach the dynamic braking design case.

Wing Loads

The wing loads were generated in a manner similar to that for the fuselage, except that aerodynamic loads are included in the force summation post-processing. The scaled vertical shear and scaled

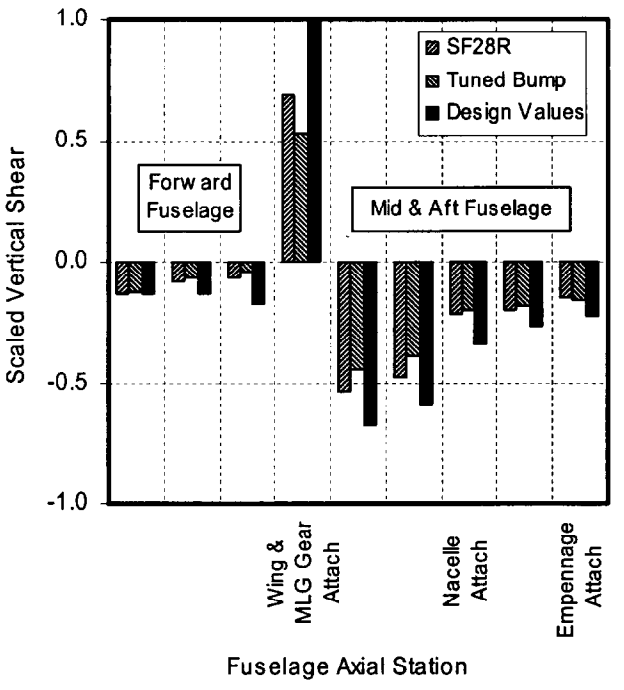

(a) shear, FZ

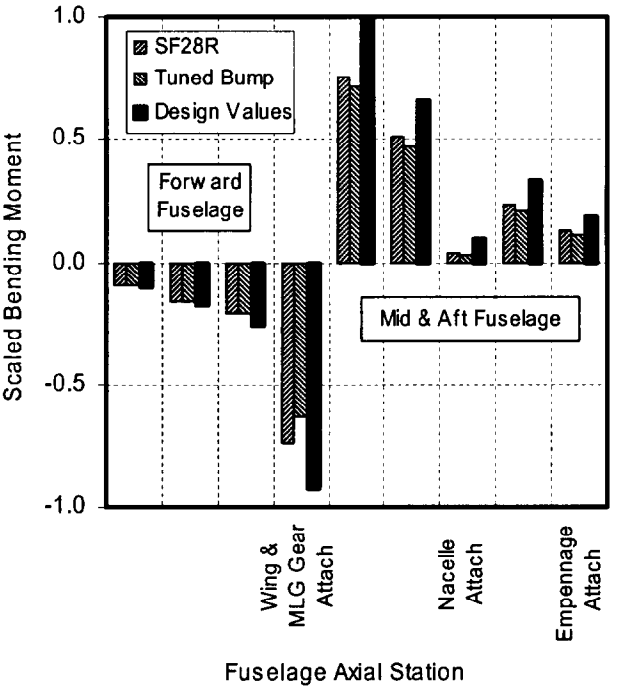

(b) bending moment, MY

Fig. 9 - Fuselage loads from taxi conditions compared against design conditions.

bending moment generated by the taxi runs are shown to be well below the respective design values in Fig. 10.

Nacelle Loads

The large business jet aircraft in this study has two fuselage mounted nacelles. Nacelle loads were generated similarly to the fuselage loads. Aerodynamic loads were assumed to be negligible. Figure 11 shows that the magnitude of the limit nacelle loads generated by dynamic taxi loads are well below the magnitude of the design values.

Additional comparisons were performed on the horizontal tail (not shown). The limit loads produced by the dynamic taxi runs were shown to be far below the design levels.

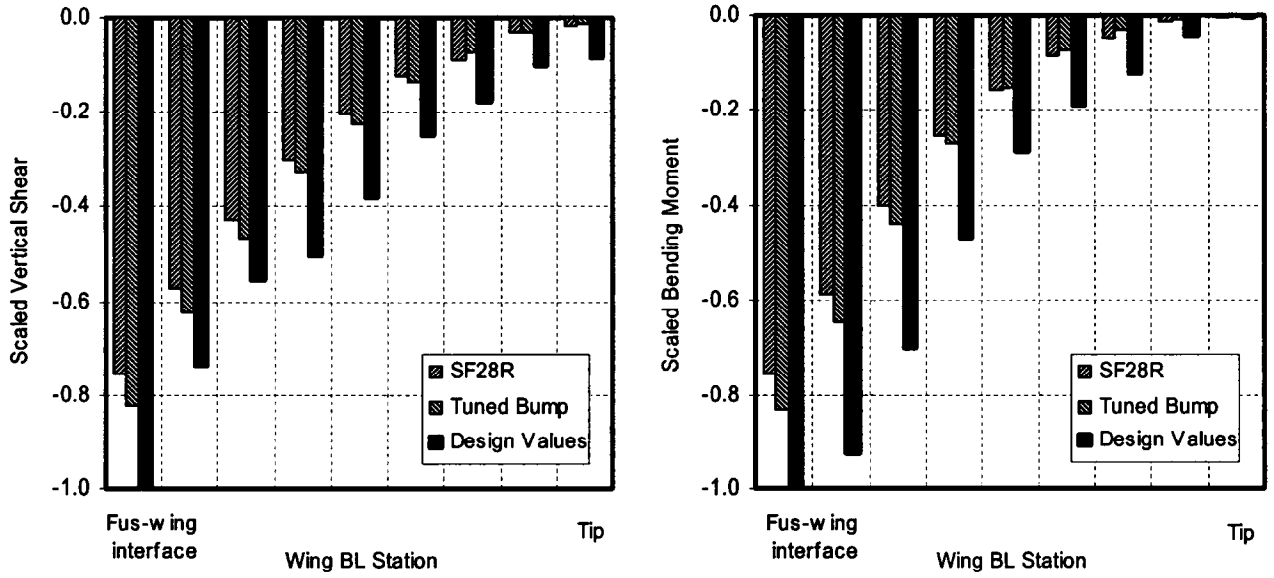

(a) shear, FZ **(b) bending, MX**

Fig. 10 - Wing loads generated from taxi conditions compared against design conditions.

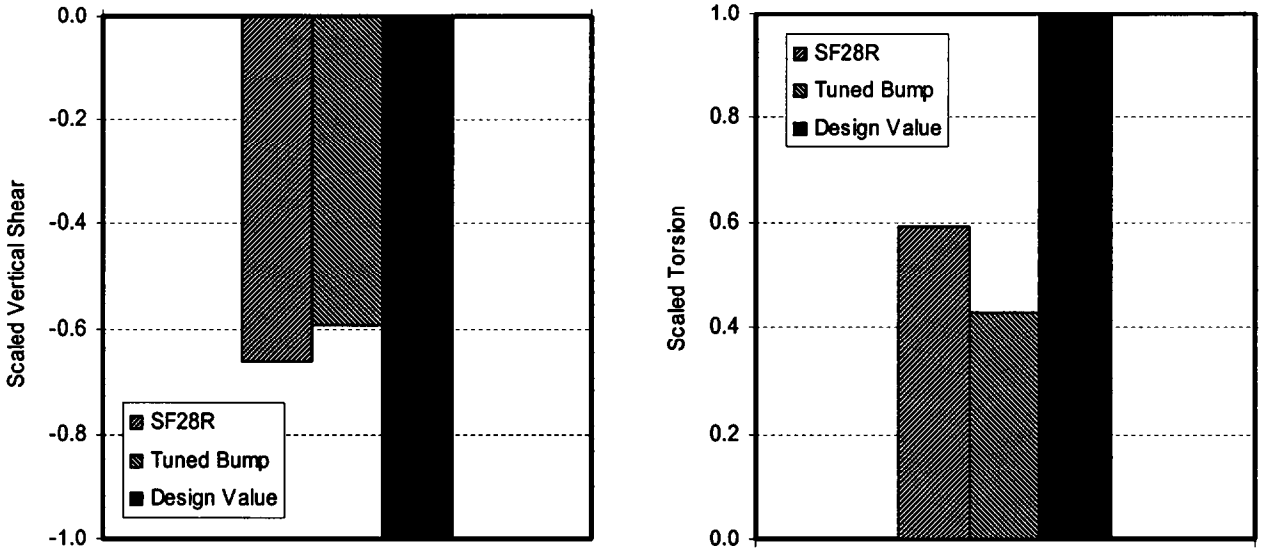

(a) shear, FZ **(b) torsion, MY**

Fig. 11 - Nacelle loads generated from taxi runs compared against design conditions.

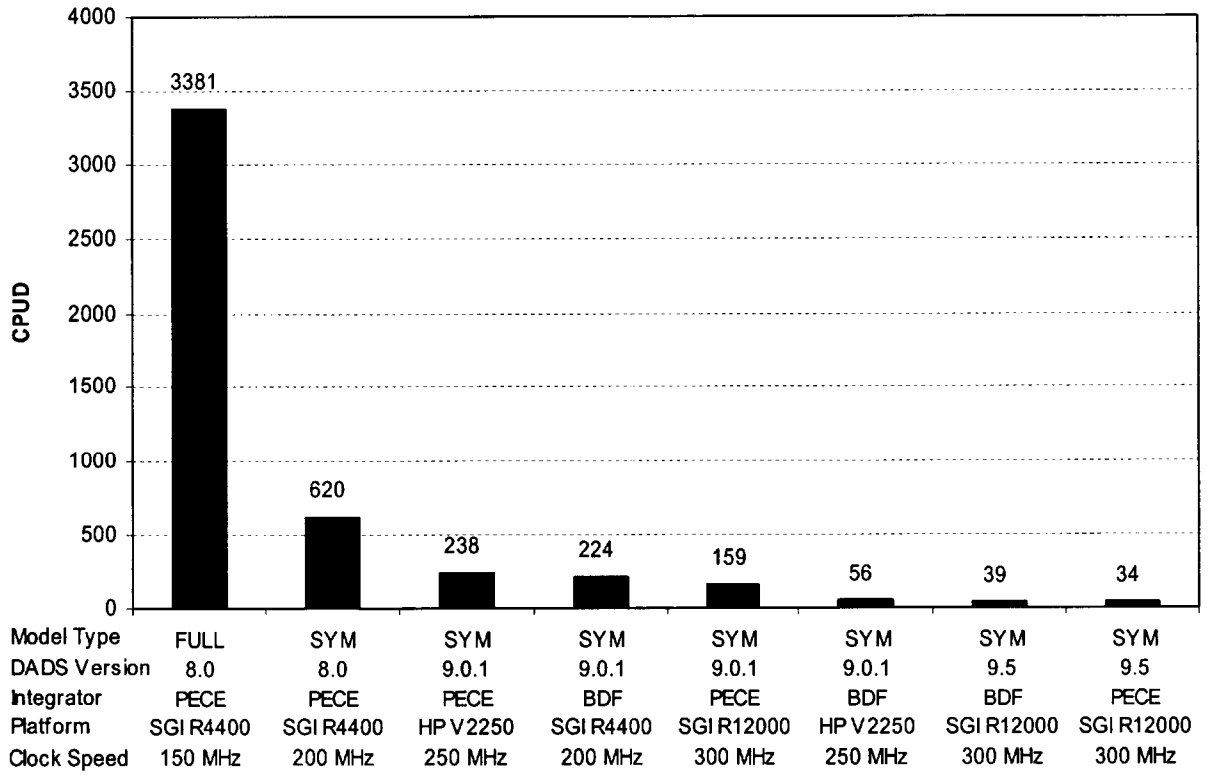

Figure 12 - Comparison of CPUD for Dynamic Taxi Runs

Simulation Performance

Although the primary focus of the paper addresses the construction of a taxi model and the results generated from the SF28R and tuned bump runs, a brief discussion on run times experienced for taxi simulations should be given. Figure 12 shows CPU-dot (CPUD), the clock-time required to complete one second of taxi simulation, for a variety of DADS integrators and computer platforms utilized throughout the course of this study. The first simulations (using a full-span aircraft model) were performed on a SGI R4400 (150 MHz) using DADS rev. 8.0, which required approximately 1 hour to complete 1 second of simulation. Therefore, 20 knot, bi-directions runs on the San Francisco runway required approximately 1 week to complete.

By reducing the full-span model to a symmetric half-model and through platform upgrades, CPUD was reduced by nearly an order of magnitude. The recent release of DADS (rev. 9.5) includes an implicit integrator (BDF) and a revamped explicit integrator (PECE) which both show a great deal of promise in reducing CPUD much further. In preliminary runs on a SGI Octane R12000, CPUD has been reduced to 34 seconds per 1 second of simulation using the PECE integrators.

As far as the dynamic taxi results reported in this paper, the runs were performed on a 200 MHz SGI using the PECE integrator. With this platform/integrator combination, the San Francisco runs required an estimated 5 million time steps to satisfy the runway profile analysis requirement of the AC, or about one month of CPU time. The tuned bump runs required only 160,000 time steps (≈1 CPU day), or about 3% of the total required for the San Francisco analysis.

Comments

It is apparent from the preceding section that dynamic taxi simulations require a considerable amount of time to complete, particularly the bi-directional runs on the San Francisco runway. It is also apparent that for the large business jet considered, the dynamic taxi conditions do not design the airframe or fuselage mounted nacelles, only the landing gear.

An alternative approach would be to use a more rigorous tuned bump analysis (perhaps with more wavelengths to consider, or some other modifications to generate higher nose gear loads) in lieu of the San

Francisco runway requirement. The tuned bump requires only a fraction of the time required for the runway profile condition. In addition, critical speeds can be readily evaluated for tuned bumps, as opposed to performing a large number of cases on the San Francisco runway to find a worst case rigid body phasing with respect to the severe bump.

Summary

The proposed AC for taxi, takeoff, and landing roll loads sets forth acceptable means of compliance for dynamic analyses using runway and double tuned bump ground profiles. Once the final AC is published, it will be necessary for all future FAA/JAA Part 25 aircraft to perform the dynamic analyses set forth in this AC or some alternative dynamic analysis deemed to be acceptable by the regulators.

The methodology used to assemble a large business jet taxi model was presented. The model consists of landing gear and flexible airframe models validated by drop test and ground vibration tests, respectively. The landing gear and airframe models were mated in DADS, a commercially available non-linear dynamic software package.

The maximum main gear load was generated with the tuned double tuned bump ($\lambda=2L$) at a critical speed determined to excite the fundamental rigid body motion of the aircraft. The maximum main gear load produced by the tuned bump is slightly higher than produced on the San Francisco runway. The maximum nose gear load was generated on the San Francisco runway on the severe bump, and is slightly higher than that obtained with double tuned bumps. The severe bump is a 12 ft discrete structure on the 7760 ft mirrored runway.

The limit gear loads produced by dynamic taxi analyses are the design cases for the large business jet aircraft considered.

The fuselage, wing, and nacelle limit loads produced by the San Francisco runway and the tuned bump are comparable in magnitude. The dynamic taxi limit airframe loads are significantly lower than the design values generated by flight or other ground handling conditions. The only exception is in the forward fuselage, where the dynamic taxi loads approach those produced by the dynamic braking condition.

The dynamic taxi simulations, especially those on the San Francisco runway, require a significant amount of time to complete due to the large number of time steps required. Unlike those produced with San Francisco, the tuned bump runs are quick, well-behaved, and exhibit peaks at speeds that can be computed prior to performing the runs.

Only with a high-performance computer coupled with a state-of-the-art integrator can these analyses be completed in an acceptable amount of time.

Acknowledgments

The authors would like to acknowledge Mr. Jack Hagelin and Mr. Mike Green of the Boeing Commercial Airplane Group for numerous enlightening telecons regarding dynamic taxi analyses. The authors would like to thank Mr. David Cross of the FAA for providing background information on the San Francisco runway. In addition, the authors would like to thank Mr. John Laughlin and Mr. Ron Hickenbottom of LMS/CADSI® for providing support related to the use of the PECE and BDF integrators for dynamic taxi analyses.

References

(1) Draft Advisory Circular 25.491-1, "Taxi, Takeoff, and Landing Roll Design Loads", available in electronic format from FAA website: `http://www.faa.gov/avr/air/acs/draftach.htm`.

(2) Tung, C.C., Penzien, J., and Horonjeff, R., "The Effect of Runway Unevenness on the Dynamic Response of Supersonic Transports", NASA CR-119, Oct. 1964.

(3) Hall, A.W., "Three-Track Runway and Taxiway Profiles Measured at International Airports C and D", NASA TN D-5703, March 1970

(4) Potter, D.M., "Measurements of Runway Roughness of Four Commercial Airports", NACA RM L56I26.

(5) International Civil Aviation Organization (ICAO) Annex 14, *Aerodromes* , Volume 1, Specification 9.4.15, p. 110, July 1996.

(6) Advisory Circular 150/5370-13, "Offpeak Construction of Airport Pavements Using Hot-Mix Ashpalt", pp. 12-17, Aug. 1990.

(7) United States Air Force Guide Specification AFGS-87221A, p. 105, June 1990.